Dynamics of microcavity exciton polaritons in a Josephson double dimer

Christine Khripkov,[1] Carlo Piermarocchi,[2] and Amichay Vardi[1]
[1]*Department of Chemistry, Ben Gurion University of the Negev, Beer Sheva 84105, Israel*
[2]*Department of Physics and Astronomy, Michigan State University, East Lansing, Michigan 48824, USA*
(Received 23 July 2013; revised manuscript received 14 November 2013; published 10 December 2013)

We study the dynamics of exciton polaritons in a double-well configuration. The system consists of two weakly coupled Bose-Josephson junctions, each corresponding to a different circular polarization of the polaritons, forming a Josephson double dimer. We show that the Josephson oscillation between the wells is strongly coupled to the polarization rotation and that, consequently, Josephson excitation is periodically exchanged between the two polarizations. Linearized analysis agrees well with numerical simulations using typical experimental parameters.

DOI: 10.1103/PhysRevB.88.235305 PACS number(s): 71.36.+c, 03.75.Lm, 03.75.Mn, 71.35.Lk

I. INTRODUCTION

Recent experiments on microcavity exciton polaritons[1] have reported coherent oscillations and quantum self-trapping characteristic of Bose Josephson junctions, highlighting the quantum fluid behavior of these quasiparticles.[2] Double-quantum-well systems in these semiconductor devices were realized using coupled micropillars[3,4] or by exploiting natural well width fluctuations that lead to a weak confinement for polaritons.[5] Several theoretical investigations anticipated these effects and pointed out the richness of the dynamics that can be observed in these inherently out-of-equilibrium systems.[6–10] One feature of microcavity polaritons is the presence of an *intrinsic* Josephson effect,[9] resulting from the coupling of left- and right-circularly polarized polaritons through an optical anisotropy term deriving from disorder or anisotropies in the microcavity structure.[11]

The simultaneous and coupled dynamics of left-right well and left-right polarization of polaritons naturally realizes a Josephson double dimer,[12–15] which represents a minimal system to explore fundamental questions such as the emergence of thermodynamics in small quantum systems.[12] A polariton-based double dimer is particularly interesting because it allows for fine control of the initial-state preparation by a spatial and polarization shaping of the pulses, and it realizes a high-temperature (compared to atoms), truly mesoscopic system. Moreover, ellipsometry measurements can provide a complete characterization of the polarization dynamics in the two wells.

Signatures of polarization precession were observed in Ref. 3. However, a comprehensive picture of the coupling between interwell Josephson oscillations and polariton polarization precession has not been obtained either experimentally or theoretically. In this work we apply the formalism of Refs. 12–14 and extend it to account for the finite polariton lifetime in order to provide a detailed weak-excitation Josephson analysis of the exciton-polariton model proposed in Refs. 9 and 10, and characterize its oscillation modes. Our main finding is that the intrapolarization Josephson oscillations (i.e., spatial oscillations of the same polarization species between the wells) and the interpolarization Josephson oscillations (i.e., polarization rotation within the wells) are in fact strongly coupled. Specifically, we study the case of strong intrapolarization coupling and weak interpolarization coupling. Under such conditions, the two bosonic Josephson junctions corresponding to the two circular polarizations of the polaritons exchange Josephson excitations ("josons") as well as particles.[12] Since the particle and joson oscillations are also coupled by the nonlinear frequency shifts, we find the natural frequencies of the collective particle-joson oscillation. The obtained frequencies agree well with numerical simulations using characteristic experimental parameters.

Polaritons possess an inherent nonequilibrium nature due to their finite lifetime. We will show, however, that the radiative recombination of the polaritons does not affect the coherence of the two coupled oscillations or contribute to renormalization of the oscillation eigenfrequency. In addition, the internal spin structure of the polaritons is robust to spin decoherence processes since the nonradiative dark-exciton states corresponding to $J_z = \pm 2$ are spectrally separated from the polariton states with $J_z = \pm 1$.

In Sec. II we describe the double-dimer model and its spin representation. The natural Josephson modes of the linearized motion are given in Sec. III, with reference to the analogous mechanical systems of nonrigid coupled pendulums. The effect of losses is considered in Sec. IV. In Sec. V we compare the theoretical closed-form predictions of the previous sections to numerical simulations, thus verifying the validity of the analysis. We conclude in Sec. VI.

II. BOSE-HUBBARD MODEL AND PSEUDOSPIN REPRESENTATION

We model the polariton double-well system using the Bose-Hubbard tight-binding four-mode model of two weakly coupled dimers,

$$\hat{H} = \left(-\frac{\Omega}{2}\sum_{\sigma}\hat{a}^{\dagger}_{\sigma,L}\hat{a}_{\sigma,R} - \frac{\omega}{2}\sum_{\alpha}\hat{a}^{\dagger}_{+,\alpha}\hat{a}_{-,\alpha} + \text{H.c.}\right) + U\sum_{\sigma,\alpha}\hat{n}_{\alpha,\sigma}(\hat{n}_{\alpha,\sigma}-1), \quad (1)$$

where $\hat{a}_{\sigma,\alpha}$ are the annihilation operators for quasiparticles with circular polarization $\sigma = \pm$ in a well, $\alpha = \{L,R\}$, Ω and ω are, respectively, the intrapolarization and interpolarization coupling frequencies, and U corresponds to the exciton-polariton interaction strength. We neglect the biexcitonic interaction between different polarizations in the same microcavity[9,10] and assume that $\Omega \gg \omega$, in agreement with current experimental conditions.[3]

We map Hamiltonian (1) into a spin problem[16] by ordering $(\hat{a}_{+,L},\hat{a}_{+,R},\hat{a}_{-,R},\hat{a}_{-,L}) \leftrightarrow (\hat{a}_1,\hat{a}_2,\hat{a}_3,\hat{a}_4)$ and defining 15 SU(4) generators $\hat{u}_{j,k} \equiv \hat{a}_k^\dagger \hat{a}_j + \hat{a}_j^\dagger \hat{a}_k$, $\hat{v}_{j,k} \equiv (\hat{a}_k^\dagger \hat{a}_j - \hat{a}_j^\dagger \hat{a}_k)/i$, and $\hat{w}_l = \sqrt{2/[l(l+1)]}(\sum_{j=1}^{l} \hat{n}_j - l\hat{n}_{l+1})$, with $1 \leqslant k < j \leqslant 4$, $1 \leqslant l \leqslant 3$, and $\hat{n}_j \equiv \hat{a}_j^\dagger \hat{a}_j$. Constructing a pseudospin vector $\hat{\mathbf{S}} = (\hat{u}_{2,1},\hat{u}_{3,2},\hat{u}_{4,3},\hat{u}_{3,1},\hat{u}_{4,2},\hat{u}_{4,1},\hat{v}_{2,1},\ldots,\hat{v}_{4,1},\hat{w}_1,\hat{w}_2,\hat{w}_3)$ from these generators [in analogy to $\mathbf{S} = (u,v,w)$ for a two-level system], we obtain

$$\hat{H} = -\frac{\Omega}{2}(\hat{S}_1 + \hat{S}_3) - \frac{\omega}{2}(\hat{S}_2 + \hat{S}_6) + \frac{U}{2}\left(\hat{S}_{13}^2 + \hat{S}_{14}^2 + \hat{S}_{15}^2\right), \tag{2}$$

where we have eliminated a $UN(N/4-1)$ c-number term which does not affect the dynamics.

The pseudospin representation (2) offers two advantages over the models used in Refs. 9, 10, and 12–14. First, by being a theory for the reduced single-particle density matrix $\hat{a}_i^\dagger \hat{a}_j$, it offers a more comprehensive description of non-Hamiltonian loss processes than phenomenological loss terms do in the Hamiltonian equations for the amplitudes $\hat{a}_i$. For example, the finite lifetime of the polaritons τ is accounted for here by solving the master equation for the N-polariton density matrix $\hat{\rho}$,

$$i\frac{d\hat{\rho}}{dt} = [\hat{H},\hat{\rho}] + i\mathcal{L}\hat{\rho}, \tag{3}$$

with the Lindblad operator

$$\mathcal{L} = -\frac{\gamma}{2}\sum_{j=1}^{4}(\hat{a}_j^\dagger \hat{a}_j \hat{\rho} + \hat{\rho}\hat{a}_j^\dagger \hat{a}_j - 2\hat{a}_j \hat{\rho} \hat{a}_j^\dagger), \tag{4}$$

where $\gamma = 1/\tau$. The dynamical equations for the S_i operators thus read

$$\begin{aligned} i\dot{\hat{S}}_i = &-\frac{\Omega}{2}\sum_{j=1,3}\sum_{k=1}^{15} c_{ij}^k \hat{S}_k - \frac{\omega}{2}\sum_{j=2,6}\sum_{k=1}^{15} c_{ij}^k \hat{S}_k \\ &+ U\sum_{j=13}^{15}\sum_{k=1}^{15} c_{ij}^k \frac{\hat{S}_j\hat{S}_k + \hat{S}_k\hat{S}_j}{2} - i\gamma\hat{S}_i, \end{aligned} \tag{5}$$

where c_{ij}^k are SU(4) structure constants.

The second benefit of the pseudospin model is didactic. It allows us to present the results in terms of generalized Bloch/Poincaré spheres where mean-field classical dynamics corresponds to motion on their surface and a decrease in reduced purity due to entanglement is reflected by penetration into their interior. We make use of this pedagogical advantage by extracting the reduced SU(2) representations for the two Bose-Hubbard dimers with circular polarization $\sigma = \pm$ from the SU(4) pseudospin as $\hat{\mathbf{S}}_+ = (\hat{S}_1,\hat{S}_7,\hat{S}_{13})$ and $\hat{\mathbf{S}}_- = (\hat{S}_3, -\hat{S}_9, \sqrt{1/3}\hat{S}_{14} - \sqrt{2/3}\hat{S}_{15})$, where the corresponding particle number in each polarization is $\hat{N}_{+(-)} = \hat{n}_{1(4)} + \hat{n}_{2(3)}$. We thus obtain two Bloch/Poincaré vectors $\mathbf{s}_\sigma = \langle\hat{\mathbf{S}}_\sigma\rangle/|\langle\hat{\mathbf{S}}_\sigma\rangle|$, where $s_{\sigma,z}$ corresponds to the normalized spatial population imbalance within the polarization σ and $s_{\sigma,x}$ and $s_{\sigma,y}$ correspond, respectively, to the real and imaginary parts of the pertinent spatial coherence.

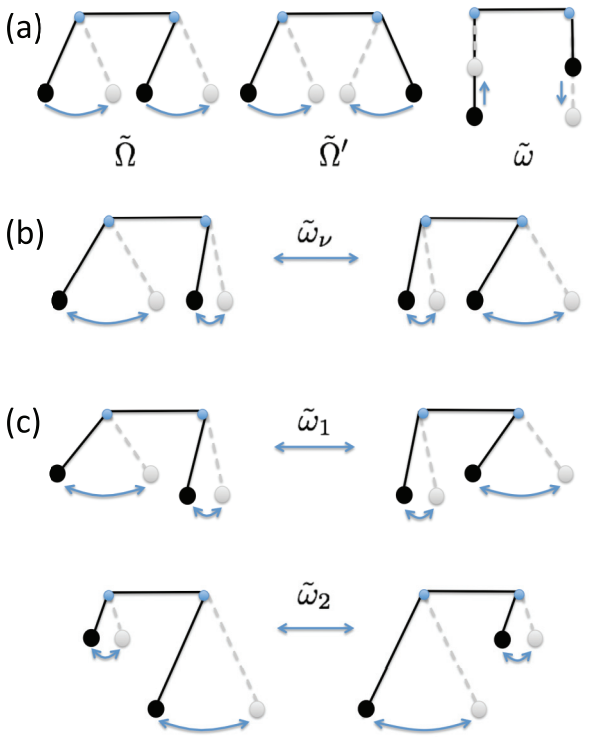

FIG. 1. (Color online) Josephson oscillation modes of an exciton-polariton double-well condensate. Each pendulum represents a double-well Bose-Josephson junction with a different circular polarization. (a) Bogoliubov modes: antisymmetric (left), symmetric (middle), and slow interpolarization (right) oscillations. (b) Slow exchange of Josephson excitation (josons) between the polarizations. (c) Natural adiabatic modes consisting of the combined exchange of particles and Josephson excitations between polarizations: opposite-phase particle and joson oscillations with dominant energy transfer (top, $\tilde{\omega}_1$) and in-phase particle and joson oscillations with dominant polarization transfer (bottom, $\tilde{\omega}_2$).

III. MECHANICAL EQUIVALENT AND JOSEPHSON OSCILLATION MODES

The low-energy spectrum for each of the two weakly coupled Bose-Hubbard dimers with different polarizations consists of harmonic-oscillator levels with Josephson frequency spacing $\tilde{\Omega}_\sigma = \sqrt{\Omega(\Omega + 2UN_\sigma)}$.[17] The four-mode system in this linear regime is thus equivalent to coupled nonrigid pendulums which can exchange their length, corresponding to the number of particles in each dimer $N_\sigma \equiv \langle\hat{N}_\sigma\rangle$, as well as their oscillation amplitude, corresponding to the excitation of each oscillator. The degree of this Josephson excitation is quantified by the respective *number of josons*,

$$\nu_\sigma = \frac{E_\sigma - E_{\sigma,g}}{\tilde{\Omega}_\sigma} = \frac{1}{\tilde{\Omega}_\sigma}\left[-\frac{\Omega}{2}\langle\hat{S}_{\sigma,x}\rangle + \frac{U}{2}\langle\hat{S}_{\sigma,z}^2\rangle + \frac{\Omega N_\sigma}{2}\right], \tag{6}$$

where E_σ and $E_{\sigma,g} = -\Omega N_\sigma/2$ denote, respectively, the energy and ground-state energy of dimer σ. While the total number of josons $\nu = \nu_+ + \nu_-$ is not strictly conserved, conservation of energy implies it is an adiabatic invariant in the linear regime.

The Bogoliubov linearized collective-oscillation modes for Hamiltonian (2) are illustrated in Fig. 1(a). In agreement with the coupled-pendulum analogy, they include (i) an antisymmetric mode at the single-pendulum frequency $\tilde{\Omega} = \sqrt{\Omega(\Omega + UN)}$, where the spatial oscillations of the two polarizations are in phase, (ii) a symmetric mode with spatial oscillations of opposite phase in the two polarizations at frequency $\tilde{\Omega}' = \sqrt{(\Omega + \omega)(\Omega + \omega + UN)}$, and (iii) slow particle oscillations between the two polarizations, maintaining a fixed total population N, with frequency

$$\tilde{\omega} = \sqrt{\omega(\omega + UN)}. \tag{7}$$

The beating of the two fast Bogoliubov modes at the difference frequency $\omega_\nu = \tilde{\Omega}' - \tilde{\Omega} \approx (\omega/\tilde{\Omega})(\Omega + UN/2)$ corresponds to the slow exchange of josons between the two polarizations [Fig. 1(b)]. As shown in Refs. 12–14 using a series of Holstein-Primakoff[18] and Bogoliubov transformations, this beat mode serves as an independent adiabatic oscillation mode whose frequency is modified as

$$\tilde{\omega}_\nu = \sqrt{\omega_\nu(\omega_\nu + U_\nu \nu)} \tag{8}$$

by the effective attractive interaction between josons $U_\nu = -(U/4)(4\Omega + UN)/(\Omega + UN)$.

The proper description of the exciton-polariton bosonic Josephson system is thus in terms of two Bose-Hubbard dimers of different polarizations which can exchange both particles and excitations. This is a far more intricate picture than the prevalent view of independent, noncoupled modes for spatial/extrinsic oscillations and polarization/intrinsic oscillations. Furthermore, the particle oscillations (at frequency $\tilde{\omega}$) and excitation oscillations (at frequency $\tilde{\omega}_\nu$) are also coupled because the frequency of oscillation within each polarization depends on the number of polaritons in it. Using the mechanical analogy, the pendulum frequencies change as they exchange their length. The effective particle-joson coupling is $U_c = (U/2)(\Omega/\tilde{\Omega})\sqrt{N\nu}$. Consequently, the final oscillation modes involve both particle and joson exchange. Diagonalization of the effective Hamiltonian for coupled particle and joson oscillators eventually yields the natural frequencies,[12–14]

$$\tilde{\omega}^2_{1,2} = \frac{\tilde{\omega}^2 + \tilde{\omega}^2_\nu}{2} \mp \left[\left(\frac{\tilde{\omega}^2 - \tilde{\omega}^2_\nu}{2}\right)^2 + \frac{\omega\omega_\nu \Omega U^2 N\nu}{\Omega + UN}\right]^{1/2}. \tag{9}$$

The two natural slow modes are shown in Fig. 1(c). The slower oscillation at frequency $\tilde{\omega}_1$ constitutes predominantly energy exchange (i.e., joson oscillations) accompanied by small population oscillations. The particle and joson oscillations in this mode are of opposite phase; that is, the joson imbalance $\Delta\nu \equiv \nu_+ - \nu_-$ is maximized when the particle imbalance $\Delta N \equiv N_+ - N_-$ is at the minimum. By contrast the faster mode at frequency $\tilde{\omega}_2$ has dominant particle oscillations accompanied by minor joson oscillations. In this case, particles and josons oscillate in phase.

IV. EFFECT OF LOSSES

The loss mechanism described in Eq. (3) with the Lindbladian (4) and a polariton lifetime of 33 ps was used in Ref. 3 to accurately describe the experimental observations for coupled micropillars. Dephasing times for exciton-polariton systems are of the order of hundreds of picoseconds and are consequently neglected. Since the loss Lindbladian equally dampens populations and coherences, it does not produce any frequency shifts other than the change in the chemical potential incurred by the decay of $N(t)$ and $\nu(t)$. The natural frequencies of Eq. (9) thus slowly vary in its presence as

$$\tilde{\omega}_{1,2} \to \tilde{\omega}_{1,2}(N(t), \nu(t)) - i\gamma, \tag{10}$$

with $N(t) = N(0)e^{-t/\tau}$ and $\nu(t) = \nu(0)e^{-t/\tau}$.

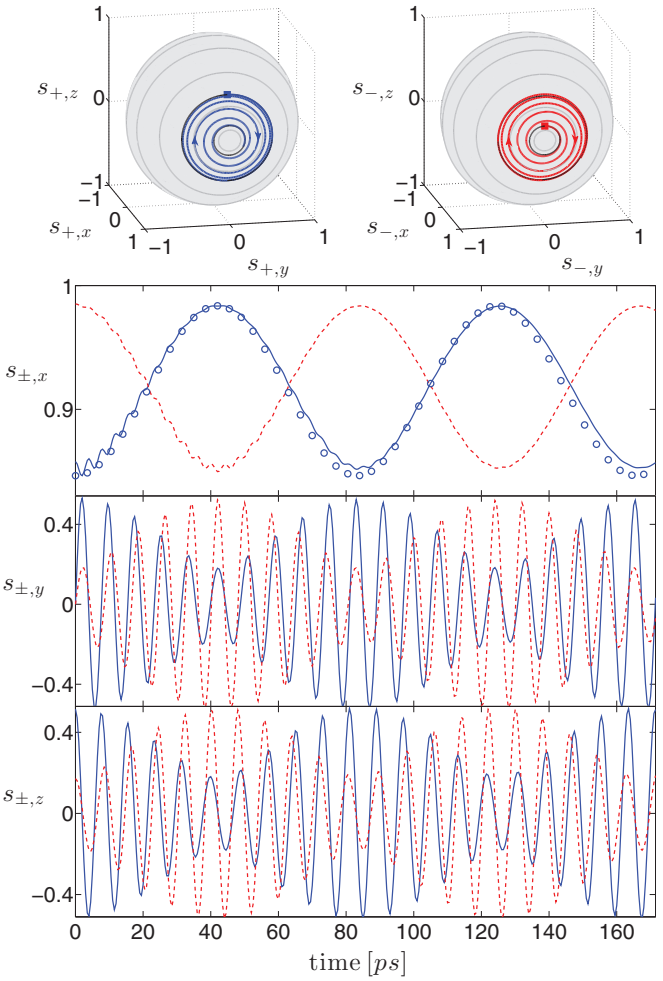

FIG. 2. (Color online) Exchange of Josephson excitations between polarizations. (top) Mean-field evolution of the reduced Bloch vectors $\mathbf{s}_+$ (left) and $\mathbf{s}_-$ (right). Symbols mark the initial state. (bottom) Components of $\mathbf{s}_+$ (solid blue line) and $\mathbf{s}_-$ (dashed red line). Circles mark oscillation at the loss-corrected frequency $\tilde{\omega}_1(t)$. Parameters are $U = 0.1\ \mu$eV, $\Omega = 500\ \mu$eV, $\omega = 50\ \mu$eV, $\tau = 50$ ps, $N = 500$, $\nu = 20$. Initial conditions correspond to $\Delta N = -13.6$ and $\Delta\nu = 16$ with zero-relative phase between polarizations and between the spatial components of each polarization, designed to excite the $\tilde{\omega}_1$ collective oscillation. The number of particles at the end of the simulation is $N \sim 16$.

V. NUMERICAL RESULTS

In order to assess the experimental feasibility of observing composite particle-joson oscillations between the

polarizations of an exciton-polariton condensate in a double-well potential, we carry out numerical simulations with characteristic experimental parameters. The tunnel coupling between the confined polaritonic ground states is taken to be $\Omega = 500\ \mu$eV, and the polarization splitting is $\omega = 50\ \mu$eV. The interaction constant is $U = 0.1\ \mu$eV,[8,9] and the number of polaritons is $N = 500$. The characteristic interaction parameters are thus $u_\Omega = 2UN/\Omega = 0.2$ and $u_\omega = 2UN/\omega = 2$. The polariton lifetime is estimated as $\tau = 50$ ps.

For the linear regime studied in this work, a classical mean-field solution in which the operators $\hat{\mathbf{S}}$ are replaced by c numbers $\mathbf{S}$ provides an accurate description of the quantum system. We have verified this approximation by conducting full quantum numerical simulations at the same values of the interaction parameters $u_{\Omega,\omega}$, obtaining excellent agreement for the duration of the simulation with particle number $N \sim 50$. Since quantum fluctuations diminish as $1/N$, the quantum-classical agreement would even improve for $N = 500$ (where quantum calculations are precluded due to computational limitations).

In Fig. 2 we plot the time evolution of the reduced Bloch vectors $\mathbf{s}_\pm$ with a preparation designed to excite the $\tilde{\omega}_1$ collective mode: Both the relative phase between the two polarizations and the internal relative phases of the two dimers are set to zero, with an initial population (particle) and energy (joson) imbalance of opposite signs. As expected, we observe an exchange of energy between the two polarizations, wherein the amplitude of the internal Josephson oscillations slowly alternates between the spheres at the expected frequency $\tilde{\omega}_1$. The resulting interpolarization population and energy oscillations are shown in Fig. 3 with the π phase difference between them and the larger joson oscillation amplitude expected for this composite natural mode.

We compare the joson-particle oscillations observed here with Fig. 2 of Ref. 9. In these numerical calculations it

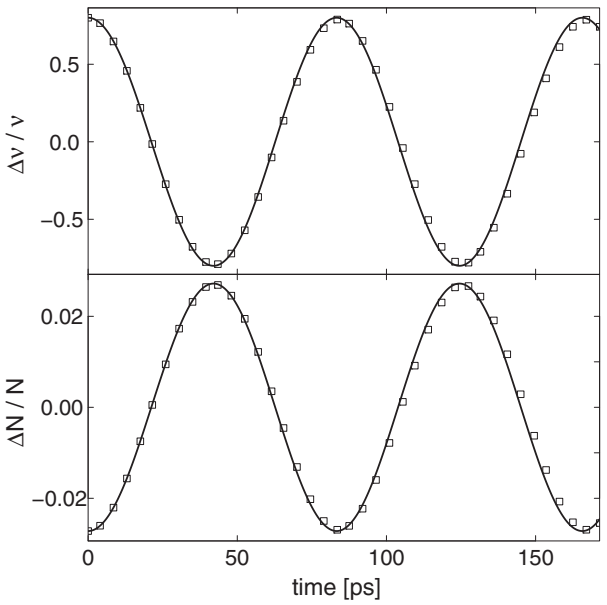

FIG. 3. Dynamics of the normalized joson imbalance $\Delta\nu/\nu$ and particle imbalance $\Delta N/N$ between the two polarizations for the parameters and preparation of Fig 2. Squares denote oscillations at the loss-corrected frequency $\tilde{\omega}_1$.

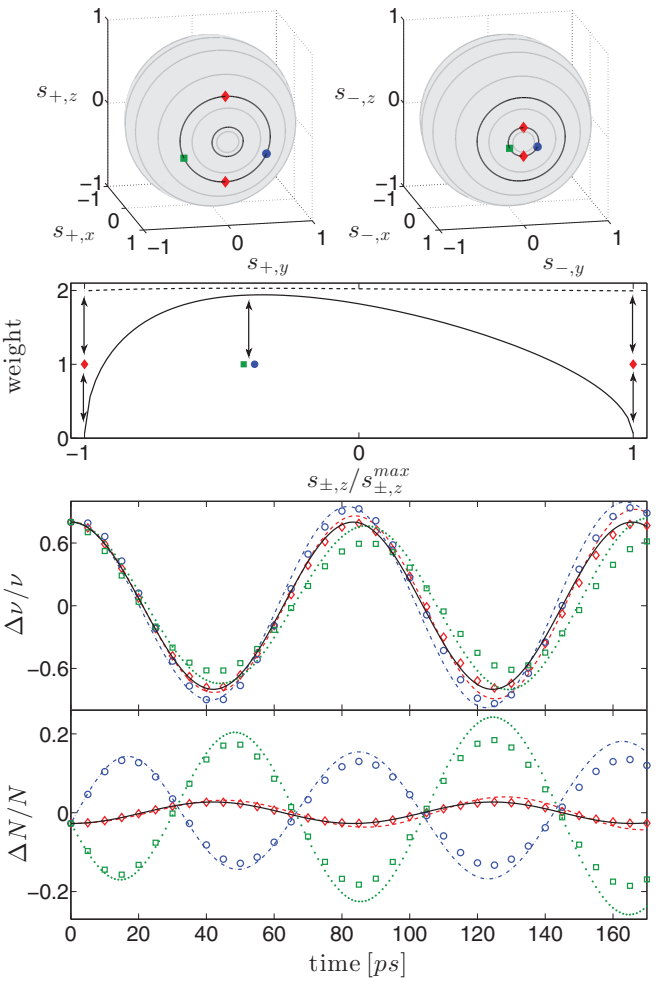

FIG. 4. (Color online) Comparison of different preparations with the same initial $\Delta N, \Delta\nu$ as in Fig. 3. (top) The initial reduced Bloch vectors $\mathbf{s}_\pm(t = 0)$. (middle) Weights (not normalized) of the $\tilde{\omega}_1$ mode (dashed) and $\tilde{\omega}_2$ mode (solid) as a function of the relative intrapolarization particle imbalance $s_{\pm,z}/s^{\max}_{\pm,z}$, where $s^{\max}_{\pm,z}$ is the maximum value of $s_{\pm,z}$ within the fixed $\Delta N, \Delta\nu$ subspace. (bottom) Dynamics of particle and joson imbalance. Parameters are the same as in Fig. 2. Symbols are numerical mean-field results, whereas lines depict the pertinent combination of slow natural-mode oscillations at $\tilde{\omega}_{1,2}$, with the weights from the middle panel.

was assumed that $\omega = 0$, so that the two polarization dimers are uncoupled. The resulting dynamics is thus the sum of two independent Josephson oscillations, and there is neither particle exchange nor energy exchange between polarizations. In the perturbative regime spatial beating is observed due to the different interaction shifts in the Josephson frequencies of differently populated polarization dimers. Larger spatial imbalances lead to self-trapping in either or both polarization dimers, depending on the preparation.

By contrast, here we only consider the Josephson-oscillation perturbative regime but have finite coupling ω between polarizations, leading to true four-mode Josephson dynamics with both population and energy flowing back and forth from one polarization to the other. Moreover, this flow is nontrivial, with the more populated polarization carrying less excitation for the $\tilde{\omega}_1$ oscillation mode depicted in Figs. 2

and 3 but with opposite behavior for the $\tilde{\omega}_2$ mode. An experiment resolving the two polarizations should easily detect the predicted effect.

In Fig. 4 we compare the mean-field evolution of various preparations which have the same initial interpolarization population and energy differences. While the preparation in which all four mode amplitudes have the same phase excites purely the $\tilde{\omega}_1$ oscillation, other preparations excite also the $\tilde{\omega}_2$ mode. The degree of this mode mixing is determined purely by the internal population imbalance within the polarizations $s_{\pm,z}$. Good agreement is obtained with the adiabatic natural-mode analysis,[12–14] which we have modified to include losses.

VI. CONCLUSION

The dynamics of exciton-polariton Josephson junctions is more complex than that of independent intrapolarization and interpolarization Josephson oscillators. Indeed the natural slow modes for interpolarization oscillations involve both particle oscillation and energy oscillation through the exchange of intrapolarization Josephson excitation. Furthermore, these slow modes are coupled, resulting in natural frequencies which involve both particle and excitation exchange. Numerical simulations with typical parameters of semiconductor microcavity systems, including radiative-recombination losses, indicate that such behavior can be observed within current experimental measurement times.

ACKNOWLEDGMENTS

We gratefully acknowledge valuable discussions with James Anglin, Doron Cohen, and Martin Strzys. This research was supported by the the United States–Israel Binational Science Foundation (BSF Grant No. 2008141) and the Israel Science Foundation (ISF Grant No. 346/11).

[1] V. Savona, C. Piermarocchi, A. Quattropani, P. Schwendimann, and F. Tassone, Phase Transitions **68**, 169 (1999).
[2] I. Carusotto and C. Ciuti, Rev. Mod. Phys. **85**, 299 (2013).
[3] M. Abbarchi, A. Amo, V. G. Sala, D. D. Solnyshkov, H. Flayac, L. Ferrier, I. Sagnes, E. Galopin, A. Lemaitre, G. Malpuech, and J. Bloch, Nat. Phys. **9**, 275 (2013).
[4] M. Galbiati, L. Ferrier, D. D. Solnyshkov, D. Tanese, E. Wertz, A. Amo, M. Abbarchi, P. Senellart, I. Sagnes, A. Lemaitre, E. Galopin, G. Malpuech, and J. Bloch, Phys. Rev. Lett. **108**, 126403 (2012).
[5] K. G. Lagoudakis, B. Pietka, M. Wouters, R. André, and B. Deveaud-Plédran, Phys. Rev. Lett. **105**, 120403 (2010).
[6] M. Wouters and I. Carusotto, Phys. Rev. Lett. **99**, 140402 (2007).
[7] M. Wouters, Phys. Rev. B **77**, 121302 (2008).
[8] D. Sarchi, I. Carusotto, M. Wouters, and V. Savona, Phys. Rev. B **77**, 125324 (2008).
[9] I. A. Shelykh, D. D. Solnyshkov, G. Pavlovic, and G. Malpuech, Phys. Rev. B **78**, 041302 (2008).
[10] D. D. Solnyshkov, R. Johne, I. A. Shelykh, and G. Malpuech, Phys. Rev. B **80**, 235303 (2009).
[11] Ł. Kłopotowski, M. D. Martin, A. Amo, L. Vina, I. A. Shelykh, M. M. Glazov, G. Malpuech, A. V. Kavokin, and R. Andre, Solid State Commun. **139**, 511 (2006).
[12] M. P. Strzys and J. R. Anglin, Phys. Rev. A **81**, 043616 (2010).
[13] M. P. Strzys and J. R. Anglin, Phys. Rev. A **85**, 053610 (2012).
[14] M. P. Strzys and J. R. Anglin, Phys. Scr. T **151**, 014046 (2012).
[15] C. V. Chianca and M. K. Olsen, Phys. Rev. A **83**, 043607 (2011).
[16] I. Tikhonenkov, J. R. Anglin, and A. Vardi, Phys. Rev. A **75**, 013613 (2007).
[17] M. Chuchem, K. Smith-Mannschott, M. Hiller, T. Kottos, A. Vardi, and D. Cohen, Phys. Rev. A **82**, 053617 (2010).
[18] T. Holstein and H. Primakoff, Phys. Rev. **58**, 1098 (1940).